ISSN 1063-7710, Acoustical Physics, 2019, Vol. 65, No. 1, pp. 1–6. © Pleiades Publishing, Ltd., 2019.

CLASSICAL PROBLEMS OF LINEAR ACOUSTICS AND WAVE THEORY

An Acoustic Metamaterial Lens for Acoustic Point-to-Point Communication in Air[1]

Fei Sun[a, b, *], Shuwei Guo[b], Borui Li[b], Yichao Liu[b], and Sailing He[b, c, **]

[a] *Key Lab of Advanced Transducers and Intelligent Control System, Ministry of Education and Shanxi Province, College of Physics and Optoelectronics, Taiyuan University of Technology, Taiyuan, 030024 China*

[b] *Centre for Optical and Electromagnetic Research, Zhejiang Provincial Key Laboratory for Sensing Technologies, JORCEP, East Building #5, Zhejiang University, Hangzhou , 310058 China*

[c] *Department of Electromagnetic Engineering, School of Electrical Engineering, Royal Institute of Technology (KTH), Stockholm, S-100 44 Sweden*

**e-mail: sunfei@zju.edu.cn*

***e-mail: sailing@kth.se*

Received March 14, 2018; Revised June 29, 2018; Accepted August 28, 2018

Abstract—Acoustic metamaterials have become a novel and effective way to control sound waves and design acoustic devices. In this study, we design a 3D acoustic metamaterial lens (AML) to achieve point-to-point acoustic communication in air: any acoustic source (a speaker) in air enclosed by such an AML can produce an acoustic image where the acoustic wave is focused (the field intensity is at a maximum, and the listener can receive the information), while the acoustic field at other spatial positions is low enough that listeners can hear almost nothing. Unlike a conventional elliptical reflective mirror, the acoustic source can be moved around inside our proposed AML. Numerical simulations are given to verify the performance of the proposed AML.

Keywords: acoustic metamaterials, focusing, Eaton lens

DOI: 10.1134/S1063771019010111

INTRODUCTION

Acoustic metamaterials are made by artificial units on the sub-wavelength orders, which can manipulate the propagation of acoustic waves in an unprecedented way [1–5]. Many novel acoustic phenomena and devices have been proposed, and later experimentally demonstrated by acoustic metamaterials, including negative mass density and modulus [6–9], anisotropic mass density [10], acoustic beam shifter [11], acoustic cloaking [12–16], acoustic super-resolution imaging [17, 18], acoustic wave rotator [19], acoustic concentrator [20], acoustic absorber [21, 22], acoustic rainbow trapping [20, 23], acoustic lens [25–27], etc.

Point-to-point communication is a relatively safe communication method. Point-to-point communication can be achieved easily through light waves or microwaves, which has been used in laser communication systems [28], mobile phones, and telephone communication. However, it is challenging to achieve a point-to-point communication using acoustic waves due to the diffraction of acoustic waves. In most cases, when one speaker is talking, all audiences around him can receive the acoustic information. Acoustic point-to-point communication often requires conversion of the acoustic signal to other kinds of signals (e.g. an electrical signal, in the case of cell phones), achieving point-to-point transmission with the help of the other signals, and finally converting it back to the acoustic signal. Can we create a special environment in which point-to-point acoustic communication can be achieved directly, without any conversion to and from other kinds of signals? In this study, we try to achieve a direct point-to-point acoustic communication by enclosing a circular region of air with an acoustic metamaterial lens (AML). The basic idea is shown in Fig. 1. The AML (colored), filled with the designed inhomogeneous media, is set around the room (a circular air region (colored white)). The small circle in the air represents the speaker, while the other small circles in the air all represent listeners. Of all the possible locations of the speaker in the room, there is only one fixed spatial location where a listener can receive the acoustic signal well (the intensity of the acoustic field here is large enough to be recognized). Listeners in other spatial locations cannot receive the information, as the intensity of the acoustic wave is below the human ear hearing range (below 20 dB) in these

[1] The article is published in the original.

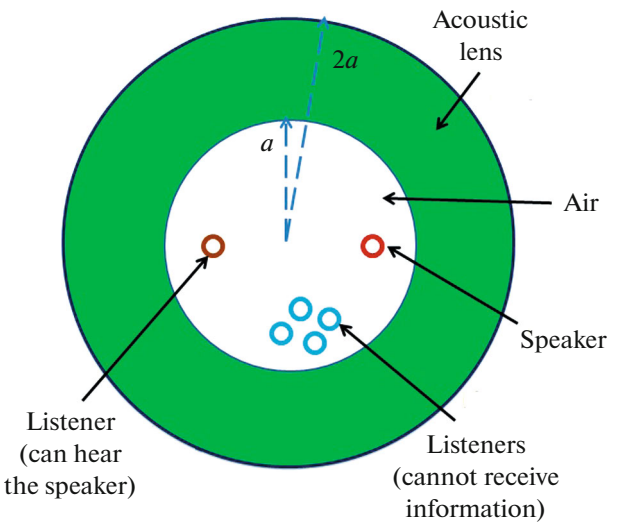

Fig. 1. Basic scheme to achieve a direct point-to-point acoustic communication in air by an AML (colored; $a < |\mathbf{r}| < 2a$). The inner white circle ($|\mathbf{r}| < a$) is air.

regions. The key to achieving such an effect is to design the AML around the room.

METHOD

We will first theoretically show what types of inhomogeneous acoustic media can achieve such an effect by making an analogy to the design of inhomogeneous media for electromagnetic waves, and then design an acoustic metamaterial structure (layered media composed of air, petroleum, and hydrogen with a gradual filling factor) based on effective medium theory to realize such an acoustic lens. The propagation of a time-harmonic acoustic velocity potential in a source-free space obeys the Helmholtz equation [29]:

$$\Delta\phi(\mathbf{r}) + \frac{\rho(\mathbf{r})\omega^2}{\kappa(\mathbf{r})}\phi(\mathbf{r}) = 0, \tag{1}$$

where ϕ is the velocity potential, ρ is the mass density, ω is the angular frequency, and κ is the modulus. The speed of the acoustic wave can be defined by

$$v = \sqrt{\frac{\kappa(\mathbf{r})}{\rho(\mathbf{r})}}. \tag{2}$$

We can rewrite Eq. (1) by introducing the speed of the acoustic wave in Eq. (2):

$$\Delta\phi(\mathbf{r}) + \frac{\omega^2}{v^2}\phi(\mathbf{r}) = 0. \tag{3}$$

Considering the propagation of electromagnetic waves in inhomogeneous media:

$$\Delta\psi(\mathbf{r}) + n^2\frac{\omega^2}{c^2}\psi(\mathbf{r}) = 0, \tag{4}$$

where ψ is the electric field, n is the refractive index of the medium, and c is speed of light in vacuum. The inside-out Eaton lens is an absolute optical imaging device, which can achieve point-to-point sharp imaging for electromagnetic waves [30–32]. The inside-out Eaton lens is a variant of Eaton lens, which can be designed by Hamiltonian optics [33]. Eaton lenses have been experimentally demonstrated at the microwave frequency range as retro-reflectors [34]. Submitting the required refractive index of inside-out Eaton lens into wave equation for electromagnetic waves (Eq. (4)), we have:

$$\begin{cases} \Delta\psi(\mathbf{r}) + \dfrac{\omega^2}{c^2}\psi(\mathbf{r}) = 0, |\mathbf{r}| \le a, \\ \Delta\psi(\mathbf{r}) + \left(\dfrac{2a}{|\mathbf{r}|} - 1\right)\dfrac{\omega^2}{c^2}\psi(\mathbf{r}) = 0, a < |\mathbf{r}| \le 2a. \end{cases} \tag{5}$$

a is a constant indicating the inner boundary of inside-out Eaton lens ($2a$ is the outer boundary of the lens). Since the forms of the acoustic wave equation (Eq. (3) and the scalar electromagnetic wave equation (Eq. (5)) are the same, we would expect that for some inhomogeneous acoustic media whose modulus and mass density vary like a special lens that works for acoustic waves, their function on acoustic waves should be the same as their function on electromagnetic waves. Combining Eqs. (2), (3) and (5), the modulus and mass density of the acoustic inside-out Eaton lens should satisfy

$$\sqrt{\frac{\kappa(\mathbf{r})}{\rho(\mathbf{r})}} = \begin{cases} v_0, |\mathbf{r}| \le a \\ \dfrac{v_0}{\sqrt{\dfrac{2a}{|\mathbf{r}|} - 1}}, a < |\mathbf{r}| \le 2a. \end{cases} \tag{6}$$

Now we have obtained the required lens (Eq. (6)) with an inhomogeneous ratio of the modulus and mass density to achieve point-to-point acoustic communication in Fig. 1. v_0 is the acoustic speed in air and $|\mathbf{r}|$ is the radial distance from the center of the inside-out Eaton lens. a is the radius of the inner air region and $2a$ is the outer radius of the colored annular region in Fig. 1. Note that there is a rigid boundary at $|\mathbf{r}| = 2a$. Another requirement on the modulus and mass density of this acoustic lens is the impedance match condition (the impedance of the lens should match the air's impedance):

$$\rho(\mathbf{r})v(\mathbf{r}) = \rho_0 v_0. \tag{7}$$

The impedance condition Eq. (7) determines the transmittance between the air region and our lens. If Eq. (7) is satisfied, energy produced by acoustic source can enter our acoustic lens without being reflected (the highest efficiency can be achieved). Combing Eqs. (2), (6) and (7), we can obtain the required mass density distribution of the impedance-matched, acoustic inside-out Eaton lens:

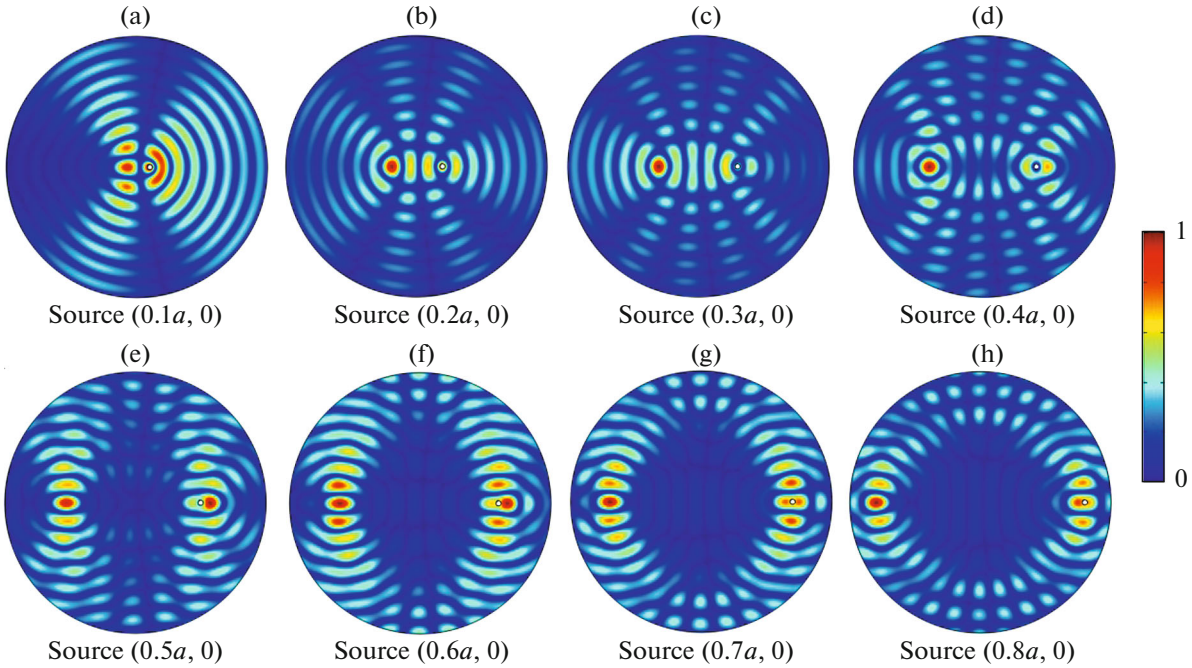

Fig. 2. 2D numerical simulation results. We only plot the normalized acoustic pressure distribution in the center air region of the impedance-matched acoustic inside-out Eaton lens. The mass density and modulus are given by Eqs. (8) and (9), respectively. From (a) to (h), as the position of the acoustic source changes from the center to the edge, the focused acoustic image changes accordingly. We choose $a = 1$ m, $\rho_0 = 1.29$ kg/m^3, $v_0 = 340$ m/s, and wavelength $\lambda_0 = 0.25$ m in all simulations.

$$\rho(\mathbf{r}) = \begin{cases} \rho_0, |\mathbf{r}| \le a, \\ \rho_0 \sqrt{\dfrac{2a}{|\mathbf{r}|} - 1}, a < |\mathbf{r}| \le 2a. \end{cases} \quad (8)$$

Putting Eq. (8) into Eq. (6), we can obtain the required modulus of the impedance-matched acoustic inside-out Eaton lens:

$$\kappa(\mathbf{r}) = \begin{cases} \rho_0 v_0^2, |\mathbf{r}| \le a, \\ \dfrac{\rho_0 v_0^2}{\sqrt{\dfrac{2a}{|\mathbf{r}|} - 1}}, a < |\mathbf{r}| \le 2a. \end{cases} \quad (9)$$

We use the commercial software COMSOL Multiphysics 5.0, based on the finite element method, to verify the performance of the acoustic inside-out Eaton lens. The performance of the impedance-matched acoustic inside-out Eaton lens, whose mass density and modulus are given in Eqs. (8) and (9), is shown in Fig. 2. If the colored annular medium ($a < |\mathbf{r}| < 2a$) is filled by acoustic materials with the modulus and mass density given in Eqs. (8) and (9), and the white circle region ($|\mathbf{r}| < a$) is filled with air, any vibration source at (x_0, y_0) in air can produce a focused acoustic image at $(-x_0, -y_0)$. In other words, we can achieve point-to-point acoustic communication between (x_0, y_0) and $(-x_0, -y_0)$ by the acoustic lens given in Eqs. (8) and (9). To make the acoustic pressure level below 20 dB in other regions (except the image point), we adjust the amplitude of acoustic source, rescale the color bar, and plot the acoustic pressure level distribution in Fig. 3.

REALIZATION DESIGN

Next, we will show how to use layered media (air, petroleum, and hydrogen) to realize the required medium in Eqs. (8) and (9). Figure 4a is a schematic diagram of our AML composed by air (medium *A*), petroleum (medium *B*), and hydrogen (medium *C*). Based on the effective medium theory [35–37], the effective mass density and modulus of the layered media (see Fig. 4b) can be given by

$$\begin{cases} \dfrac{1}{\rho_\parallel} = \dfrac{f_A}{\rho_A} + \dfrac{f_B}{\rho_B} + \dfrac{f_C}{\rho_C}, \\ \rho_\perp = f_A\rho_A + f_B\rho_B + f_C\rho_C, \\ \dfrac{1}{\kappa} = \dfrac{f_A}{\kappa_A} + \dfrac{f_B}{\kappa_B} + \dfrac{f_C}{\kappa_C}, \end{cases} \quad (10)$$

where $f_A = d_A/d, f_B = d_B/d$ and $f_C = d_C/d$ are filling factors ($f_A + f_B + f_C = 1$, $0 < f_i < 1$, $i = A, B, C$). We choose air, petroleum, and hydrogen as media *A*, *B* and *C*, respectively. The modules of these media are $\kappa_A = v_0^2\rho_0 \sim 1.42 \times 10^5$ Pa, $\kappa_B = 1.2382 \times 10^9$ Pa and $\kappa_C = 0.95 \times 10^9$ Pa. The mass densities of these media are $\rho_A = 1.21$, $\rho_B = 700$, and $\rho_C = 0.09$ kg/m^3. Note that we only consider 2D case (acoustic waves are within the *x*–*y*

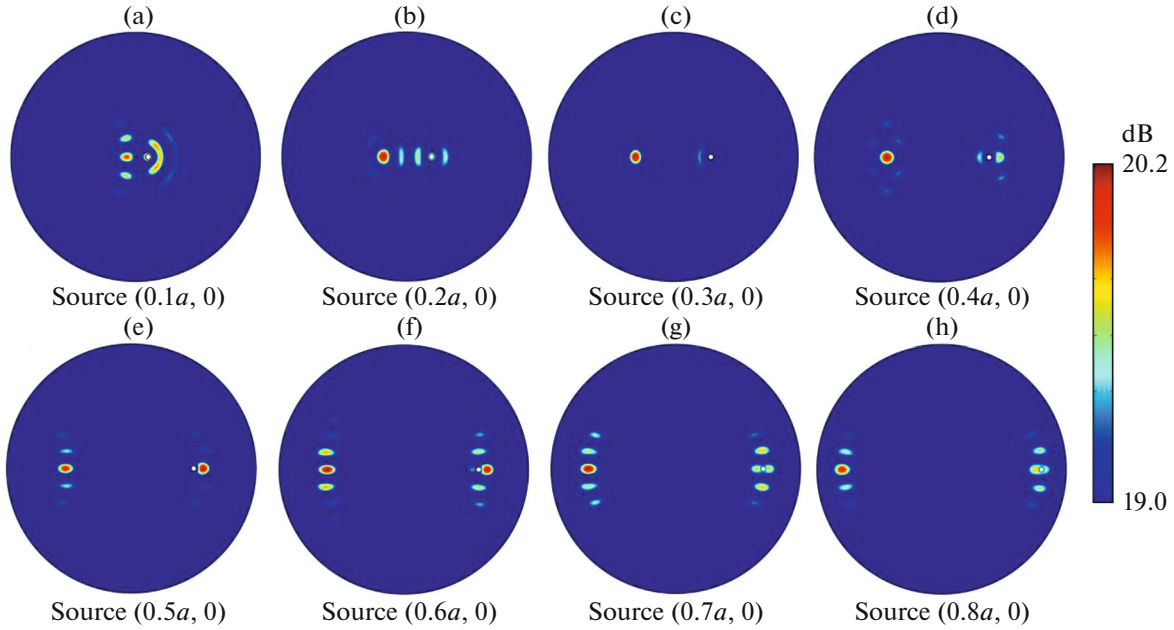

Fig. 3. 2D numerical simulation results. We plot the acoustic pressure level distribution in the center air region of the AML. Note that the amplitude of the source is adjusted, and the color bar is rescaled to make sure that the acoustic pressure level is below 20 dB in other regions (except the image point). The acoustic pressures in blue regions are below 19 dB. Only acoustic pressures in red regions are a bit larger than 20 dB. All other settings are the same as ones in Fig. 2.

plane). Therefore, only mass density within the x–y plane works. In this case, only $\rho_{\parallel}$ in Eq. (10) work (we do not need to consider $\rho_{\perp}$ in 2D case).

To realize the AML, we need first to make some simplifications: the first simplification is that the outmost boundary of the AML is chosen at $|\mathbf{r}| = 1.85a$ (we set a rigid boundary at $|\mathbf{r}| = 1.85a$) not at $|\mathbf{r}| = 2a$ due to the infinite modulus at $|\mathbf{r}| = 2a$ in Eq. (9), which cannot be realized by any materials. Numerical simulations show that this simplification does not have obvious influence on the performance of the AML (the field distribution is still almost like Fig. 2; we do not show them here). The second simplification is to divide the whole lens to seventeen different layers (see Fig. 4a), in each of which the effective mass density and modulus are constant. From the inner layer to the outer layer, we arrange a layer number, i.e. no. 1, 2, ..., 17, and the radius of each layer's inner and outer boundaries are shown in the Table. Note that the accurate calculated filling factors from Eqs. (8)–(10) at the last layer (no. 17) should be $f_B = 0.8212$, and $f_C = 0.2287$ in which the condition $f_A + f_B + f_C = 1$ and $0 < f_A < 1$ cannot be satisfied at the same time. Therefore, the third simplification is to set filling factors $f_A = 0$, $f_B = 0.8$, and $f_C = 0.2$ at the last layer (no. 17). The simplified AML is composed of seventeen layers of annular layered media with different filling factors along the z direction (see Fig. 4a). The detailed parameters of each layer are given in the Table 1. The performance of the simplified AML is shown in Fig. 5, which reflects that the simplified AML can still provide good point-to-point imaging.

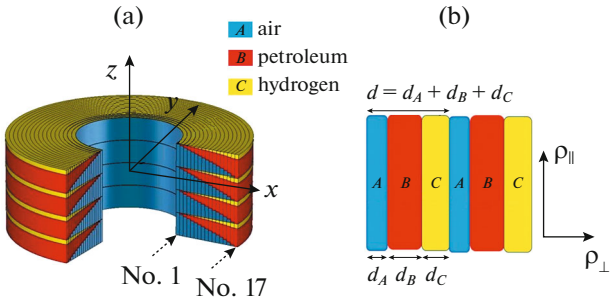

Fig. 4. (a) A schematic diagram of our 3D AML composed by air (colored blue), petroleum (colored red), and hydrogen (colored yellow); (b) the effective medium theory of layered media.

DISCUSSION AND CONCLUSIONS

Our AML is different from the echo wall, which can achieve long-distance acoustic communication with extremely small attenuation around the wall. An echo wall cannot achieve point-to-point acoustic communication (i.e. other listeners around the wall can also receive the acoustic signal). For an elliptical reflective mirror, only two focal points can achieve point-to-point acoustic communication. However, there are infinitely many spatial locations where such an effect can be achieved in our AML. Even if the speaker is moving, such an acoustic point-to-point relation still holds. Note that our AML cannot achieve

Table 1. Detailed parameters for each layer in Fig. 3a

Layer number	Inner radius [a]	Outer radius [a]	Filling factor of air f_1	Filling factor of petroleum f_2	Filling factor of hydrogen f_3	Effective mass density, kg/m^3	Effective modulus, Pa
1	1	1.05	0.9885	0.0089	0.0026	1.25814	152 896
2	1.05	1.1	0.9273	0.0622	0.0105	1.19662	160 757
3	1.1	1.15	0.868	0.1135	0.0185	1.13767	169 086
4	1.15	1.2	0.8102	0.1631	0.0267	1.08093	177 962
5	1.2	1.25	0.7535	0.2114	0.0351	1.02606	187 479
6	1.25	1.3	0.6975	0.2587	0.0438	0.97276	197 753
7	1.3	1.35	0.642	0.3051	0.0529	0.92073	208 926
8	1.35	1.4	0.5864	0.3511	0.0625	0.86972	221 181
9	1.4	1.45	0.5303	0.3969	0.0728	0.81944	234 752
10	1.45	1.5	0.4733	0.4428	0.0839	0.76961	249 949
11	1.5	1.55	0.4148	0.4892	0.096	0.71995	267 192
12	1.55	1.6	0.3538	0.5366	0.1096	0.67011	287 066
13	1.6	1.65	0.2894	0.5856	0.125	0.6197	310 418
14	1.65	1.7	0.2202	0.6369	0.1429	0.56823	338 533
15	1.7	1.75	0.1436	0.6918	0.1646	0.51506	373 477
16	1.75	1.8	0.0559	0.7521	0.192	0.45928	418 836
17	1.8	1.85	0	0.8	0.2	0.39946	481 558

a super-resolution acoustic imaging, as positive inhomogeneous media cannot amplify/convert the evanescence waves like other special lenses [17, 18].

By analogizing the wave equations between acoustic waves and electromagnetic waves in inhomogeneous media, we design an inhomogeneous acoustic lens (an inside-out Eaton lens), which can be utilized for point-to-point acoustic communication and acoustic imaging. After some simplifications, we design an AML composed of layered air, petroleum,

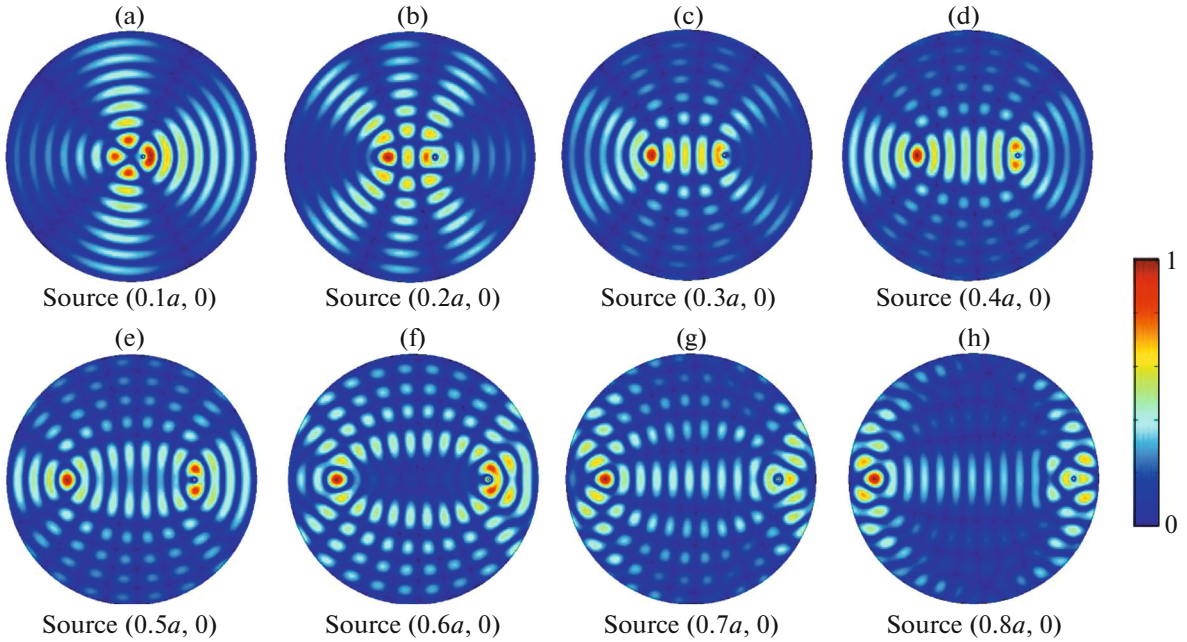

Fig. 5. 2D numerical simulation results. We plot the normalized amplitude of the acoustic pressure distribution in the simplified AML. The structure and parameters of the simplified AML are given in Fig. 4a and the Table 1, respectively. From (a) to (f), the position of the acoustic source changes from the center to the edge, its point-to-point image changes accordingly. All other settings are the same as ones used in Fig. 2.

and hydrogen to realize the acoustic inside-out Eaton lens based on the effective medium theory, whose performance is verified by numerical simulations. The proposed lens will have many potential applications in acoustic point-to-point communications, acoustic wave focusing, and acoustic imaging. The proposed theoretical method (the acousto-optic analogy method) can also be utilized to design many other novel acoustic devices.

ACKNOWLEDGMENTS

This work is partially supported by the National Natural Science Foundation of China (nos. 11604292, 11621101, 91233208 and 60990322), the Postdoctoral Science Foundation of China (no. 2017T100430), the fundamental research funds for the central universities (no. 2017FZA5001), the National Key Research and Development Program of China (no. 2017YFA0205700), the Program of Zhejiang Leading Team of Science and Technology Innovation and AOARD.

REFERENCES

1. G. Ma and P. Sheng, Sci. Adv. **2** (2), e1501595 (2016).
2. S. A. Cummer, J. Christensen, and A. Alù, Nat. Rev. Mater. **1**, 16001 (2016).
3. M. H. Lu, L. Feng, and Y. F. Chen, Mater. Today **12** (12), 34 (2009).
4. Yu. I. Bobrovnitskii, Acoust. Phys. **60** (4), 371 (2014)
5. Yu. I. Bobrovnitskii, Acoust. Phys. **61** (3), 255 (2015).
6. T. Brunet, A. Merlin, B. Mascaro, K. Zimny, J. Leng, O. Poncelet, C. Aristégui, and O. Mondain-Monva, Nat. Mater. **14** (4), 384 (2015).
7. S. H. Lee, C. M. Park, Y. M. Seo, Z. G. Wang, and C. K. Kim, Phys. Rev. Lett. **104** (5), 054301 (2010).
8. Z. Liang and J. Li, Phys. Rev. Lett. **108** (11), 114301 (2012).
9. V. A. Burov, K. V. Dmitriev, and S. N. Sergeev, Acoust. Phys. **55** (3), 298 (2009).
10. D. Torrent and J. Sánchez-Dehesa, Phys. Rev. Lett. **105** (17), 174301 (2010).
11. P. Wei, F. Liu, Z. Liang, Y. Xu, S. T. Chu, and J. Li, Europhys. Lett. **109** (1), 14004 (2015).
12. C. Faure, O. Richoux, S. Félix, and V. Pagneux, Appl. Phys. Lett. **108** (6), 064103 (2016).
13. L. Sanchis, V. M. García-Chocano, R. Llopis-Pontiveros, A. Climente, J. Martínez-Pastor, F. Cervera, and J. Sánchez-Dehesa, Phys. Rev. Lett. **110** (12), 124301 (2013).
14. S. Zhang, C. Xia, and N. Fang, Phys. Rev. Lett. **106** (2), 024301 (2011).
15. H. Chen and C. T. Chan, Appl. Phys. Lett. **91** (18), 183518 (2007).
16. S. A. Cummer and D. Schurig, D. New J. Phys. **9** (3), 45 (2007).
17. J. Zhu, J. Christensen, J. Jung, L. Martin-Moreno, X. Yin, L. Fok, X. Zhang, and F. J. Garcia-Vidal, Nat. Phys. **7** (1), 52 (2011).
18. J. Li, L. Fok, X. Yin, G. Bartal, and X. Zhang, Nat. Mater. **8** (12), 931 (2009).
19. X. Jiang, B. Liang, X. Y. Zou, L. L. Yin, and J. C. Cheng, Appl. Phys. Lett. **104** (8), 083510 (2014).
20. T. Li, M. Huang, J. Yang, Y. Li, and J. Yu, Acoust. Phys. **58** (6), 642 (2012).
21. J. Mei, G. Ma, M. Yang, Z. Yang, W. Wen, and P. Sheng, Nat. Commun. **3**, 756 (2012).
22. A. Climente, D. Torrent, and J. Sánchez-Dehesa, Appl. Phys. Lett. **100** (14), 144103 (2012).
23. J. Zhu, Y. Chen, X. Zhu, F. J. Garcia-Vidal, X. Yin, W. Zhang, and X. Zhang, Sci. Rep. **3**, 1728 (2013).
24. X. Ni, Y. Wu, Z. G. Chen, L. Y. Zheng, Y. L. Xu, P. Nayar, X. P. Liu, N. H. Lu, and Y. F. Chen, Sci. Rep. **4**, 7038 (2014).
25. F. Sun, S. Li, and S. He, J. Acoust. Soc. Am. **142**, 1213 (2017).
26. B. Li, F. Sun, and S. He, Appl. Phys. Express **10** (11), 114001 (2017).
27. B. Li, F. Sun, and S. He, Appl. Phys. Express **11** (2), 024301 (2018).
28. A. K. Majumdar, J. Opt. Fiber Commun. Rep. **2** (4), 345 (2005).
29. D. D. Reynolds, *Engineering Principles of Acoustics: Noise and Vibration Control* (Allyn & Bacon, 1981).
30. Q. Wu, X. Feng, R. Chen, C. Gu, S. Li, H. Li, Y. Xu, Y. Lai, B. Hou, H. Chen, and Y. Li, Appl. Phys. Lett. **101** (3), 031903 (2012).
31. Y. Zeng and D. H. Werner, Opt. Express **20** (3), 2335 (2012).
32. J. C. Miñano, Opt. Express **14**, 9627 (2006).
33. U. Leonhardt and T. Philbin, *Geometry and Light: The Science of Invisibility* (Dover Publ., 2010).
34. Y. G. Ma, C. K. Ong, T. Tyc, and U. Leonhardt, Nat. Mater. **8** (8), 639 (2009).
35. Y. Cheng, F. Yang, J. Y. Xu, and X. J. Liu, Appl. Phys. Lett. **92** (15), 151913 (2008).
36. M. Schoenberg and P. N. Sen, J. Acoust. Soc. Am. **73** (1), 61 (1983).
37. S. Rytov, Sov. Phys. Acoust. **2**, 68 (1956).